JAERI-M
90-175

COMMENTS ON DISSIPATIVE DRIFT WAVE TURBULENCE AND L-H TRANSITION

October 1990

Hiroshi AIKAWA

日本原子力研究所
Japan Atomic Energy Research Institute

JAERI-Mレポートは，日本原子力研究所が不定期に公刊している研究報告書です。
入手の問合わせは，日本原子力研究所技術情報部情報資料課（〒319－11茨城県那珂郡東海村）あて，お申しこしください。なお，このほかに財団法人原子力弘済会資料センター（〒319-11茨城県那珂郡東海村日本原子力研究所内）で複写による実費頒布をおこなっております。

JAERI-M reports are issued irregularly.
Inquiries about availability of the reports should be addressed to Information Division, Department of Technical Information, Japan Atomic Energy Research Institute, Tokai-mura, Naka-gun, Ibaraki-ken 319-11, Japan.

編集兼発行　日本原子力研究所
印　　刷　日立高速印刷株式会社

JAERI-M 90-175

Comments on Dissipative Drift Wave Turbulence and L-H Transition

Hiroshi AIKAWA

Department of Thermonuclear Fusion Research
Naka Fusion Research Establishment
Japan Atomic Energy Research Institute
Naka-machi, Naka-gun, Ibaraki-ken

(Received September 12, 1990)

It is shown that the diffusion coefficients due to the dissipative drift wave turbulence, which have been described by several authors in the different forms corresponding to the turbulence strength, can be written as a unified form by introduing a parameter representing the turbulence strength. Therefore, the model of L-H transition whose cause was pointed out to be possibly the dissipative drift wave turbulence by the author previously[1], can be found to be rewritten in a simpler form which consistently covers wholly the discussions developed in the previous report[1].

Keywords : Plasma, Dissipative Drift Wave, Turbulence, Tokamak, L-H Transition

散逸性ドリフト波乱流とＬ－Ｈ遷移に関するコメント

日本原子力研究所那珂研究所核融合研究部
相川　裕史

（1990年9月12日受理）

散逸性ドリフト波乱流による拡散係数は，これまでに幾人かの著者によって，それぞれ乱流の強さに応じて異なった形で記述されてきたが，乱流の強さを表わすあるパラメータを導入することによって，１つの統一された形に表わすことができることを示した。それゆえに，前に本著者により示されたようにＬ－Ｈ遷移モデルがもっと簡単な形で，前に示したレポートの内容を矛盾なく抱括できることを示した。

那珂研究所：〒311-01　茨城県那珂郡那珂町大字向山801-1

Contents

1. Introduction and Motivation 1
2. Behaviors of the Unified Diffusion Coefficient 9
3. Relations with L-H Transition 11
4. Concluding Remarks 17
Acknowledgement 18
References 18

目　　次

1. 序論及び動機 1
2. 統一された拡散係数の様相 9
3. Ｌ－Ｈ遷移との関連 11
4. 結　　論 17
謝　　辞 18
参考文献 18

1. Introduction and Motivation

In the model of L-H transition, based on the dissipative drift wave turbulence theory, as presented in the previous report[1], it is shown that the drastic L-H transition can be induced by the sufficient condition that electron temperature (T_e) exceed the certain threshold whose value is determined by the alternation of the two governing diffusion coefficients that T_e-dependence of the diffusion coefficient varies from $\propto T_e^{5/6}$ in the low-T_e region (deduced by Kadomtsev and Pogutse[2] within the restriction of the fluid-type strong turbulence) to $\propto T_e^{-2}$ in the high-T_e region (deduced by the author, extending the turbulence theory evolved by Kadomtsev and Pogutse[2] into the region of the kinetic-type-weak turbulence) as T_e increases from a low value to a higher one, so that the diffusion coefficient increases at the initial stage according to $T_e^{5/6}$-dependence as T_e increases, though it turns to decrease at a certain threshold value of T_e, corresponding to Te^{-2}-dependence, therefore, the diffusion can be drastically improved to result in the L-H transition, with the help of the enhancement effect of the density-gradient dependence of the diffusion coefficient.

The above-mentioned two regimes are the modellized cases of turbulence, strong and weak, which are very convenient to explain such a drastic change as L-H transition. The actual case, however, might not be that. As T_e increases, the turbulence must be changed continuously from strong to weak, accompanying the continuous change of the diffusion coefficient.

Fortunately, until the present day there have been presented several formula of the diffusion coefficients concerning to the dissipative drift wave turbulence with some respective applicability limitations, besides the above-mentioned two regimes.

In the present paper, they are reconsidered from the viewpoint of the turbulence strength to expect to find a common feature which might benefit us not only to make the L-H transition mechanism physically more understandable but make the applicability of the previous report[1] better-defined.

According to Terry and Diamond[3], in the case of moderate Reynolds number (0.1~ a few) which is defined as the ratio of the parallel correlation time to the coherent nonlinear relaxation rate

by them, the diffusion coefficient is given to be

$$D_{TD} = \frac{V_*^2 r_n}{C_s} \left(\frac{\nu_{ei} C_s}{\omega_{Te}^2 r_n} \right)^{2/3} \frac{\pi}{2} \frac{1}{\hat{S}^3} \cdot C_{TD} \tag{1}$$

where $V_* \equiv \omega_*/k_\theta$, ω_*: electron diamagnetic frequency, k_θ: wave number along the poloidal direction, $r_n \equiv \left| \frac{d \ln n_e}{dr} \right|$, n_e: electron density, r: the position of the minor radius direction, $C_s \equiv \sqrt{T_e/M_i}$, T_e: electron temperature, M_i: ion mass, ν_{ei}: electron-ion collision frequency, $\omega_{Te} \equiv V_e/Rq$, $V_e \equiv \sqrt{T_e/m_e}$; m_e: electron mass, R: major radius, q: a safety factor $\hat{S} \equiv r_q'/q$, $q' \equiv dq/dr$, and C_{TD} represents the average evaluation at a mean wave number in the turbulent spectrum, being estimated to get a value around ~3 in the case of the spectrum line width of $\Delta\omega_k/\omega_* \sim 1$ by Terry and Diamond.

In the case of the limit of large Reynolds number, they present the diffusion coefficient as follows;

$$D_{TD}(R_e \to \infty) \sim \rho_s^2 C_s / r_n \tag{2}$$

where $\rho_s \equiv C_s/\Omega_i$, Ω_i: ion gyro-frequency.

Then, we should take into consideration the pseudo-classical type of the diffusion which has been empirically adopted at first and reinforced by the several numerical calculations[4], having the form of

$$D_{ps} \sim \frac{\nu_{ei} \rho_e^2}{\theta^2} C_{ps} \tag{3}$$

where ρ_e: electron gyro-radius, θ: shear parameter ($= r_n \hat{S}/qR$), and C_{ps}: a numerical factor.

In the last place, we should add in the line-up of the dissipative drift wave turbulence diffusions the two forms of the diffusion coefficients which were already mentioned in the previous report by the author[1];

$$D_{kp} \sim \frac{\nu_{ei}^{1/3} (\rho_e v_e)^{4/3}}{(r_n \theta)^{2/3} (\Omega_i \Omega_e)^{1/3}} \tag{4}$$

which is derived as a limit of the maximum of the diffusion coefficient in the strong turbulence by Kadomtsev and Pogutse[2], and

$$D_H \sim \frac{\rho_e \nu_{ei}^{5/3} a^3 \Omega_i^{1/2}}{\theta^{10/3} r_n r \Omega_e^{7/6}} \tag{5}$$

which is derived by the author as a limiting case of the weak turbulence on the basis of Kadomtsev and Pogutse-analysis, where a is a minor radius of a plasma and Ω_e is an electron gyro-frequency.

All the equations (1)-(5) represent the diffusion of the dissipative drift wave turbulence, derived from the various theoretical or experimental backgrounds. Then, what equation should we adopt in the practical use? The key to judge this question may be the turbulence strength. In the strong turbulence limit, Eqs. (2) and (4) are probably applicable candidates, especially Eq. (2) may be the strongest, then next may be Eq. (4). Eq. (1) should be the following in the turbulence strength order, of moderate Reynolds number case.

But, of the left-behind two cases (Eqs. (3) and (5)) Eq. (5) should be the weakest case. Then, Eq. (3) should be the fourth order? Originally, Eq. (3) have only the mere implication as to the turbulence strength that it should be in the case of moderate or weak turbulence though it is widely applied from the moderate Reynolds number region to the adiabatic region, so that the turbulence strength with regard to Eq. (3) and (1) cannot be all clearly distinguishable. But maybe either of Eq. (3) or (1) is the third or fourth order. Here, for the temporary convenience, we proceed the analysis, assuming that Eq. (1) is the third order, and Eq. (3) is the fourth order stength.

Then, investigating the dependence of T_e, n_e, B (a toroidal magnetic field) and r_n, we find as follows;

$$D_{TD}(R_e \to \infty) \propto T_e^{3/2}/B^2 r_n \tag{6}$$

$$D_{kp} \propto T_e^{5/6} n^{1/3}/B^{4/3} r_n^{4/3} \tag{7}$$

$$D_{TD} \propto T_e^{1/6} n_e^{2/3}/B^{2/3} r_n^{5/3} \tag{8}$$

$$D_{ps} \propto T_e^{-1/2} n_e/r_n^2 \tag{9}$$

$$D_H \propto T_e^{-2} n_e^{5/3} B^{4/3}/r_n^{13/3} \tag{10}$$

This is a very interesting result. In the first place, T_e-dependence shows the arithmetical progression of the power with the difference of (-2/3) from Eq. (6) to Eq. (9), with the exception of Eq. (10) which shows the jump of (-3/2) power difference from Eq. (9).

In the second place, n_e-dependence also shows the arithmetical progression in the power with the difference of (1/3) from Eq. (6) to Eq. (9), similarly with the exception of Eq. (10) which gives the jump of (2/3)-power difference from Eq. (9).

Similarly, B and r_n dependences also give the arithmetical progression in the power with the equal differences of (2/3) and (-1/3) respectively from Eq. (6) to Eq. (9), with the exception of Eq. (10) which gives the jumps of (4/3) and (-7/3) power differences in the cases of B and r_n respectively.

Here, it should be noticed that there is a disagreeable jump of the power progression between Eqs. (9) and (10), which, however, would be covered if the form of $D \propto T_e^{-7/6} n_e^{4/3} B^{2/3} / r_n^{7/3}$ were inserted between them, even though the defects still exist in the power progression of T_e and r_n in Eq. (10). As it were, if T_e^{-2} were replaced by $T_e^{-11/6}$ in Eq. (10), the T_e-progression would be complete, though the slight difference between (-2) and (-11/6) still remains without any interpretation. As for the r_n-dependence, the deviation from the would-be-right progression is comparatively large, as it were $r_n^{-13/3}$ in Eq. (10) should be $r_n^{-8/3}$ if the (-1/3)-power progression continues to Eq. (10).

The above-results concerning to the n_e-and T_e-dependences may be crudely interpreted as that n_e-dependence is only included in ν_{ei}, whose dependence is going up as the turbulence grow weaker, on the other hand, T_e-dependence is contained not only in the -3/2 negative power in ν_{ei}, but in the positive power in ρ_s or C_s, all combined to compete each other to give the final effect of (-2/3) power progression.

As for B-dependence, B is included in ρ_s, the characteristic length of this type of the diffusion, giving the B^{-2}-dependence in Eq. (2), though B, on the other band, makes the parallel correlation time of this turbulence effectively smaller as B grows stronger, to result in the contribution of the positive power of B.

Concerning to r_n-dependence, it should be noticed that the density gradient is originally the driving force of this type of the instability, and represented in r_n in the denominator of Eq. (2). When the tubulence becomes weak, the system is getting into the the adiabatical electron regime (the ions are getting into the kinetic region) and this adiabaticity is known to lead to make the r_n-power dependence negative in the diffusion coefficient.

Here, we arrive to note that the above-described beautiful progression indicates that a certain common nature must govern the diffusion coefficient, in accordance with the degree of the turbulence strength. Terry and Diamond[3] introduce the Reynolds number to represent the turbulence degree though it is not so simple to adopt here because it contains the nonlinear term. Waltz et al.[4], on the other hand, often use the adiabaticity, defined as $(\omega_{Te}^2 \hat{S}^2 r_n / \nu_{ei} C_s)$, to distinguish the system between the hydrodynamic regime and the adiabatic electron regime. This adiabaticity may be able to be used as a measure to represent the turbulence degree because in the hydrodynamic region, the width of the frequency spectrum induced by the nonlinear instability exceeds the parallel correlation frequency to lead the system grow into the strong turbulent state, while in the adiabatical regime, the linear instability structure can be maintained to let the system remain in the weak turbulence state because the parallel flow velocity is larger than the width of the phase velocity induced by the nonlinear instability to make the turbulence remain weak. Furthermore, Kadomtsev and Pogutse[2] introduce the quantity δ, which is equivalent with the inverse of the adiabaticity used by Waltz et al. to distinguish the system between the hydrodynamic region and the kinetic one.

Here, based on the above disscussions concerning to the relation between the adiabaticity and the turbulence level, we may think that the inverse of the adiabaticity can be adopted as a measure of the turbulence level because it can be expected to be apparently proportional to the turbulence strength though it is not rigidly proved theoretically.

Then, we try to rewrite Eqs. (1)-(5) to draw out the term of $(\nu_{ei} C_s / \omega_{Te}^2 \hat{S}^2 r_n)$ to find

$$D_{TD}(R_e \to \infty) \sim \frac{\rho_s^2 C_s}{r_n} \tag{11}$$

$$D_{KP} \sim \frac{\rho_s^2 C_s}{r_n} \left(\frac{\nu_{ei} C_s}{\omega_{Te}^2 r_n \hat{S}^2}\right)^{1/3} \tag{12}$$

$$D_{TD} \sim \frac{\rho_s^2 C_s}{r_n} \left(\frac{\nu_{ei} C_s}{\omega_{Te}^2 r_n \hat{S}^2}\right)^{2/3} \frac{\pi}{2\hat{S}^{5/3}} C_{TD} \tag{13}$$

$$D_{ps} \sim \frac{\rho_s^2 C_s}{r_n} \left(\frac{\nu_{ei} C_s}{\omega_{Te}^2 r_n \hat{S}^2}\right) C_{ps} \tag{14}$$

and

$$D_H \sim \frac{\rho_s^2 C_s}{r_n} \left(\frac{\nu_{ei} C_s}{\omega_{Te}^2 r_n \hat{S}^2}\right)^{5/3} \left(\frac{r_n}{\rho_s}\right)^{1/3} \frac{a^3}{r r_n^2} \quad . \tag{15}$$

As expected, there emerges a beautiful series of a-third power of $(\nu_{ei} C_s / \omega_{Te}^2 r_n \hat{S}^2)$ though the numerical accessaries are attached in Eqs. (13)-(15). This result shows us that the inverse of the adiabaticity can be a substitute of the turbulence strength, and, as pointed out in the previous paragraph, such a type of the diffusion coefficient as $D \sim \frac{\rho_s^2 C_s}{r_n} \left(\frac{\nu_{ei} C_s}{\omega_{Te}^2 r_n \hat{S}^2}\right)^{4/3} \propto T_e^{-7/6} n_e^{4/3} B^{2/3} r_n^{-7/3}$ is possible to exist between Eqs. (14) and (15) to make the series complete. Furthermore, looking over from Eq. (11) to Eq. (15), we notice that the power of $(\nu_{ei} C_s / \omega_{Te}^2 r_n \hat{S}^2)$ increases from 0 to 5/3. Then, we can take a step forward to speculate that the above described discrete set of the power progression may be tranformed to be a unified form of the continuous set of the power-progression representing the turbulence strength.

Therefore, in the next step, we try to find such a form of the diffusion coefficient as

$$D \sim \frac{\rho_s^2 C_s}{r_n} X^{\frac{1}{\beta + \alpha X}} \tag{16}$$

where

$$X = \frac{\nu_{ei} C_s}{\omega_{Te}^2 r_n \hat{S}^2} \tag{17}$$

and α, β are arbitrary positive factors to determine, expecting Eq. (16) to represent all the Eqs. (11)-(15). As a first step, we try to confirm that Eq. (16) is consistent with Eqs. (11)-(15). As X, representing the inverse of the adiabaticity, goes to the infinity, in other words,

the turbulence goes to the infinite limit, Eq. (16) becomes $D \sim \frac{\rho_s^2 C_s}{r_n}$ which corresponds to Eq. (11), and as X goes to the zero-limit, Eq. (16) becomes

$$D \sim \frac{\rho_s^2 C_s}{r_n} X^{\frac{1}{\beta}} \to 0 \tag{18}$$

which may be corresponding to D_H if $\frac{1}{\beta} \sim \frac{5}{3}$ (that is, $\beta \sim 0.6$) and X is very small but not zero, though the numerical accessaries in Eqs. (13)-(15) are not included in this argument. Therefore, as a second step, we try to discuss the numerical factors in Eqs. (13)-(15).

In Eq. (13), Terry and Diamond[3] estimate the factor C_{TD} around ~3 in the case of the moderate Reynolds number region with the condition that the frequency width due to the turbulence is the same order of electron diamagnetic frequency ω_*. And the mean wave number $\langle k_\theta \rangle$ is around $\sim 0.1\ \rho_s^{-1}$. They also find the energy lies predominantly in the region of the small wave number ($k_\theta \rho_s \leq 0.1$). Furthermore the quantity δ, introduced by Kadomtsev and Pogutse[2], is easily found to have an approximate form of

$$\delta \sim \frac{1}{\langle k_\theta \rho_s \rangle} \cdot \frac{\nu_{ei} C_s}{\omega_{Te} r_n \hat{S}^2} \tag{19}$$

Remembering[2] that the numerical factor of Eq. (15) is deduced from the arguments as to this quantity δ, and, furthermore, the inverse of the adiabaticity, defined as $\omega_* \nu_{ei} / k_\parallel^2 V_e^2$, is found to take the same form of δ in Eq. (19) if we take into account the facts of $\omega_* \sim k_\theta \rho_s C_s / r_n$ and $k_\parallel \sim k_\theta \Delta X \hat{S} / R_q \sim k_\theta \rho_s \hat{S} / R_q$ in case of $\Delta X \sim \rho_s$, we may replace X in Eq. (16) with δ of Eq. (19). If we do so, the difference emerges from the part of $1/\langle k_\theta \rho_s \rangle$ in Eq. (19). Therefore, if this part can explain the numerical parts of Eqs. (13)-(15) consistently, we can adopt δ instead of X. Then, we try to estimate the order of the numerical factors of Eqs. (13)-(15). As pointed in the above discussions, C_{TD} is around O(1), and the numerical factor of Eq. (15) is easily found to be $O(10) \sim O(10^2)$, and C_{ps} in Eq. (14) depends on $\langle k_\theta \rho_s \rangle$ and will be found to be around O(10) if we obey the estimation by Terry and Diamond of $\langle k_\theta \rho_s \rangle \lesssim 0.1$.

On the other hand, we can find easily $(1/k_\theta \rho_s)^{2/3} \sim 4.6$, $(1/k_\theta \rho_s) \sim 10$, and $(1/k_\theta \rho_s)^{5/3} \sim 46$ at $\langle k_\theta \rho_s \rangle \sim 0.1$, respectively, each of which would correspond to the numerical factor of Eqs. (13)-(15) if we would replace

X with δ. This ordering quite agrees well with the above-discussed estimations.

Furthermore, In cases of Eqs. (11) and (12), the estimation of $(1/k_\theta\rho_s)^0 \sim 1$, and $(1/k_\theta\rho_s)^{1/3} \sim 2.2$, is consistent with the fact that the numerical part is, in the sense of the physical meaningness, not attached in the Eqs. (11) and (12).

Then, setting $\alpha = 1$ and redefining X_o as

$$X_o = \frac{1}{\langle k_\theta\rho_s \rangle} \frac{\nu_{ei} C_s}{\omega_{Te} r_n \delta^2} = \frac{1}{\langle k_\theta\rho_s \rangle} X \tag{20}$$

we can write the unified form of the dissipative drift wave turbulence as a consequence of the physical speculation as follows;

$$D = \frac{\rho_s{}^2 C_s}{r_n} X_o^{\frac{1}{\beta+X_o}} \tag{21}$$

Here, let's estimate the value β and $\langle k_\theta\rho_s \rangle$. Equation (15) indicates that at small X_o, $1/\beta+X_o$ should take the value 5/3 but the value of the small X_o is not definite. Then we select $\beta = 0.5$ which means that $\frac{1}{\beta+X_o}$ becomes $\frac{5}{3}$ at $X_o = 0.1$ and becomes 2 at $X_o = 0$ limit. Practically, the β-value does not affect the physical behavior of Eq. (21). As for $\langle k_\theta\rho_s \rangle$, as pointed out previously, Terry and Diamond estimates $\langle k_\theta\rho_s \rangle \lesssim 0.1$, though this criterion must change corresponding to the turbulence level. But, we have no other alternative as a practical use to indicate the mean wave number than to choose a certain value below 0.1.

Here we adopt $\langle k_\theta\rho_s \rangle \sim 0.0666$, as it were $1/\langle k_\theta\rho_s \rangle = 15$ to match the numerical calculation, though the situation almost never change even if we adopt $\langle k_\theta\rho_s \rangle \sim 0.1$ only to give in the slight slide of the function $Y = X_o^{1/\beta+X_o}$ as shown later in Fig. 1 and Fig. 2.

In the next section, we investigate Eq. (21) numerically from the various viewpoints. In the third section, we investigate the relation between Eq. (21) and L-H transition. In the last section, we conclude the results.

2. Behaviors of the Unified Diffusion Coefficient

From the previous section, it is obvious that the intesesting part of Eq. (21) is the term $X_o^{1/\beta+X_o}$ which represents the contribution from the turbulence. Therefore, in Fig. 1, the function

$$Y = X_o^{\frac{1}{\beta+X_o}} \tag{22}$$

is shown with the parameters $\beta = 0.5$ and $\beta = 0$ with $<1/k_\theta\rho_s>=15$ to make the situation clearer. As described in the previous section, we treat the case of $\beta = 0.5$ and $1/<k_\theta\rho_s>=15$ as a model case. As a whole, the function Y increases approximately linearly from $X = 0$ to $X \cong 0.1$, then reaches the maximum $Y \cong 1.37$ at $X \simeq 0.2$, thereafter, goes down slowly to the ultimate limit of $Y = 1$ at $X = \infty$. This fact indicates that Y may be, roughly speaking, $\propto X$ at $X \lesssim 0.1$, and remain constant around $1 \sim 1.37$ $X \gtrsim 0.1$. In other words, below $X \sim 0.1$, the pseudo-classical type ($Y \propto X$) may be used as a practical use, and above $X \sim 0.1$, Eq. (2) may be not a wrong choice within the factor of 2. This tendency cannot be altered still in the case of $\beta = 0$, or in the case of $1/<k_\theta\rho_s> = 10$ as shown in Fig. 2, though the approximate linear part is extended to $X \sim 0.15$ in case of $1/<k_\theta\rho_s> = 10$.

Next, in order to look into the function Y more closely, we take out the power part of the function Y to envisage it in the same Figures 1 and 2. In the region below $X \lesssim 0.1$, the power part varies from 2 (at $X = 0$) to 0.5 (at $X = 0.1$). In looking more closely into the region $X \leq 0.1$, we divide the region into three parts, $0 \leq X \lesssim 0.033$, $0.033 \leq X \leq 0.066$, and $0.066 \leq X \leq 0.1$. In the first region, the base part of the function Y, as it were (15X), becomes less than 1, and the power part $(\frac{1}{0.5+15X})$ is more than unity, so that Y gets a smaller value than the base value (15X), which means that Y decreases rapidly more than the speed of the linearity. In the second region $0.033 \leq X \leq 0.066$, the base part is still smaller than unity, though the power part becomes smaller than unity, therefore, totally Y gets a more closer value to unity than the base value (15X). In other words, the linearity is weakened but it does not deviated so much from it. In the third region $0.066 \leq X \leq 0.1$, the base part turns larger than unity, and the power part grows much smaller than unity enough to reach $\frac{1}{2}$ at $X = 0.1$, and

Y begins to saturate and deviate more from the linearity.

In the case of the region $X \gtrsim 0.1$, Y experiences the maximum at $X \cong 0.21$, then goes down slowly to reach the final unity value at $X \to \infty$. Here we should remark as to the maximum point $X \cong 0.21$ where the power part of the function takes the value 1/3.65 whose value happens to be close 1/3 around which the diffusion coefficient is predicted to take the maximum value by Kadomtsev and Pogntse[2] when they deduce Eq. (4). With regard to this point, if we take $\beta = 0$, as also shown in Fig. 1, the maximum point moves to $X \cong 0.18$ whose value gives the power part of the function the value 1/2.7 which is also near the prediction by Kadomtsev and Pogutse.

The above results suggest that below $X \lesssim 0.033$, the system is in the adiabatic electron regime, governed by the diffusion coefficient with the power part of more than unity such as Eq. (3) or (5), and in the region of $0.033 \lesssim X \lesssim 0.1$, the system turns to the intermediate region of the adiabatical and hydrodynamic regimes (corresponding to the so-called moderate Reynolds number region named by Terry and Diamond), and above $X \gtrsim 0.1$, the system enters into the strong turbulent state of the hydrodynamic region.

Though the choosing way of β or $1/\langle k_\theta \rho_s \rangle$ makes the situation numerically a little ambiguous, the whole arrays of the diffusion coefficients Eqs. (1)-(5), discovered by several authors, might be possibly covered by Eq. (21) and found to be consistent with the characteristic features representing each diffusion coefficient of Eqs. (1)-(5). It is the practical use that we are interested in here, so it will be allowed to use Eq. (21) as one of the ways to get at the kernel of this type of the nonlinear turbulence when many features characterizing this type of the turbulence are consistently interpreted. But, it should be also taken into notice that the only way to prove this scenario is to calculate the exact nonlinear drift wave equation numerically or solve it analytically with the exact use of the techniques describing the turbulent state exactly.

3. Relations with L-H Transition

In the first place, we try to apply Eq. (21) to the actual experimental data as similarly as we did in Ref. 1 to demonstrate D_H and D_{kp}. Here, we borrow again the same ASDEX data[5] as we did in Ref. 1 not only to envisage L-H transition from the viewpoint of the unified form of Eq. (21) but also to compare it with the behavior of D_H and D_{kp} on the same basis.

The results are shown in Fig. 3 which is found to confirm the results of Fig. 2 in Ref. 1. In Ref. 1, D_{KP} is assumed as a representative of the strong turbulence case. That is to say, as described in Ref. 1, it is expected that in the cases of OH and L-mode plasmas, the peripheral diffusion is dominated by the strong turbulence represented by D_{KP}, while in the case of H-mode plasma, it is turned to be dominated by the weak turbulence represented by D_H. Therefore, it is proper that we compare the behavior of D_{kp} in Fig. 2 in Ref. 1 with D in Fig. 3 in the present paper in the cases of OH and L-mode plasmas, while in the case of H-mode plasma, we compare D in the case of H-mode plasma in Fig. 3 with D_H-line in the region within $\Delta r \lesssim -3.0$ cm and D_{kp}-line in the region outside $\Delta r \gtrsim -3.0$ cm in Fig. 2(c) of Ref. 1, in other words, the assumed line is D_H inside $\Delta r \lesssim -3.0$ cm, and transferred to D_{kp}-line outside $\Delta r \gtrsim -3.0$ cm at which D_H crosses over D_{kp}. Although the absolute values of the diffusion coefficient D are roughly twice larger than the results of Ref. 1, which is obviously due to not only the numerical factors $(1+T_i/T_e)^{1/3}$ or $(1+\eta_e)$ in D_{kp} or D_H in Ref. 1 which is omitted in Eqs. (1)-(5) but also the choice of $\langle k_\theta \rho_s \rangle$-value in Eq. (21), the overall tendency is found quite alike each other. That is, Fig. 3 shows that the diffusion coefficient of L-mode case is approximately twice larger than that of OH case, keeping the similar radial dependency each other, while the diffusion coefficient of H-mode case steeply decreases from the strong turbulence in the outer region ($0 \gtrsim \Delta r \gtrsim -3.0$ cm) to the weak turbulence in the inner region ($\Delta r \lesssim -3.0$cm). This fact clearly supports that the unified form of the diffusion coefficient, derived from the consistent unification of the existing several diffusion coefficients of the dissipative drift wave turbulence, is applicable to all the cases (OH, L-mode and H-mode) presented by Ref. 1 with regard to L-H transition.

Next, we seek the electron temperature threshold (T_{th}) of L-H transition as we did in Ref. 1 with the use of D_H and D_{kp} with the condition $D_H \leq D_{kp}$. Here, the procedure is simple and straightforward. The unified diffusion coefficient Eq. (21), being a function of T_e, can be differenciated with respect to T_e with the other parameters (r_n, n, B etc.) fixed. As shown in Fig. 4 as a sample of the diffusion coefficient Eq. (21) as a function of T_e, Eq. (21) is an increasing function of T_e in the region of small T_e (strong turbulence case), then reaches the maximum and decreases as T_e goes up still more (enter into the weak turbulence region). Therefore, as you see it, the threshold should be the maximum point (though we replace it later with $\frac{\partial^2 D}{\partial T_e^2} = 0$ only for the practical reason) which is determined by the condition of

$$\frac{\partial D}{\partial T_e} = 0 \tag{23}$$

This condition easily results in the value

$$X_o \simeq 0.91 \tag{24}$$

numerically when $\beta = 0.5$. (for example, when $\beta = 0$, Eq. (24) slides to $X_o \cong 1.15$) With the use of Eq. (20), Eq. (24) easily gives T_{th} in the form of

$$T_{th} = 6.65 \times 10^{-9} \frac{Z_{eff}^{1/2}}{A^{1/4}} \left(\frac{n_e}{r_n}\right)^{1/2} \left(\frac{Rq}{\hat{S}}\right) \tag{25}$$

where the units are T_{th}(eV), $n_e(m^{-3})$, r_n(m), and R(m), and both of $1/\langle k_\theta \rho_s \rangle$ and $\ln\Lambda$ are assumed to be 15. And if we assume the current probile $j = j_o(1 - \frac{r^2}{a^2})$, then Eq. (25) turns to be

$$T_{th} = 1.66 \times 10^{-2} \frac{Z_{eff}^{1/2}}{A^{1/4}} \left(\frac{n_e}{r_n}\right)^{1/2} \frac{Ba^4}{Ipr^2} \tag{26}$$

which is a much simpler form than Eq. (14) in Ref. 1.

Then we can compare Eq. (26) with T_{th} of Eq. (14)* given in Ref. 1. Regardless of the numerical factor $(1+\frac{T_i}{T_e})^{2/17}$ or $(1+\eta_e)^{6/17}$, both equations are very resembling. That is, n_e, B, I_p, Z_{eff}, A and r dependences are almost similar, only slight differences of the order of (1/17 ~ 3/17)-power. However, the exceptions are r_n and a dependences which are differing each other about the order of (1/2 ~ 1) power. The reason is quite clear. That is, in Eq. (21), we push the part of $(r_n/\rho_s)^{1/3}a^3/rr_n^2$ in Eq. (15) of D_H into the part of $1/<k_\theta\rho_s>$ which is numerically taken to be 15 in the present case. Therefore the contribution of this part is absorbed into the numerical part of Eq. (26).

Originally, the part of $(r_n/\rho_s)^{1/3}a/rr_n^2$ obviously results from how to estimate $k_\theta = m/r$ (m: mode number) which Kadomtsev and Pogutse approximate $m \sim \sqrt{a/\Delta x}$ where Δx is a localization length. Therefore, the physical difference is explained as that Eq. (26) treats $1/<k_\theta\rho_s>$ as a constant value of 15 while Eq. (14) in Ref. 1 treats it as some functions of several parameters though we make it match the numerical order in deducing Eq. (21).

The determination of $1/<k_\theta\rho_s>$, in accord with the corresponding turbulence strength, is not a easy task because it involves the nonlinear behavior of the frequency spectrum. Besides r_n and n_e dependences, the other parameter dependences of both equations (Eq. (26) and Eq. (14) in Ref. (1)) are consistent with the experimental data as discussed in Ref. 1. Therefore, n_e and r_n dependences should be examined a little more closely. In Eq. (26), T_{th} eventually does not contain n_e-dependence if $r_n = |n_e/\frac{dn_e}{dr}|$ is taken into account, while Eq. (14) in Ref. 1 depends on $n_e^{-10/17}$. The only available experimental data concerning to this respect is JET data[6], which, unfortunately, cannot tell which should be favorable because of the randomness of the data points, but appearing that both are not inconsistent.

One more remark should be added with respect to T_{th}. In deriving Eq. (26), we set the condition $\partial D/\partial T_e = 0$. But, as seen in Fig. 4, this

---

* for the convenience of the discussions, Eq. (14) in Ref. 1 is cited here

$$T_{th} = 1.66\times10^{-2}\,\frac{Z_{eff}^{8/17}n_e^{8/17}a^{82/17}B^{18/17}(1+\eta_e)^{6/17}}{A^{5/17}I_p^{16/17}r_n^{18/17}r^{38/17}(1+\frac{T_i}{T_e})^{2/17}}$$

point is the summit of the mountain-like curve of T_e, which forms a comparatively broad width of T_e around this maximum point. Therefore, it is feared that L-H transition cannot occur practically unless the T_e-rise exceeds the maximum point considerably, because the enhancing mechanism of the transition, as described in Ref. 1, can fail to work around $\partial D/\partial T_e \sim 0$. Therefore, as a practical use, it may be appropriate to take the threshold condition as

$$\frac{\partial^2 D}{\partial T_e^2} = 0 \tag{27}$$

This means the maximum point of $|\partial D/\partial T_e|$ ($\partial D/\partial T_e < 0$, discard the other maximum point in case of $\partial D/\partial T_e > 0$ which has no interests here). As an example of Fig. 4, this point corresponds to $T_e \simeq 400$ eV. The condition of Eq. (27) can be easily interpreted numerically as

$$X_o \simeq 0.42 \tag{28}$$

with the same assumptions with regard to β and $1/\langle k\theta\rho_s\rangle$ in deriving Eq. (24). The condition of Eq. (28) leads to the practical T_{th} which is only different from Eq. (26) by the numerical factor $\sqrt{0.91/0.42} \sim 1.47$,

$$T_{th}^{P} \sim 2.44 \times 10^{-2} \frac{Z_{eff}^{1/2}}{A^{1/4}} \left(\frac{n_e}{r_n}\right)^{1/2} \frac{Ba^4}{I_p r^2} \tag{29}$$

As demonstrated in Ref. 1, we can present the value of Eq. (29) in cases of the existing Tokamak machines with the assumptions $Z_{eff} = 2$, $A = 2$, $r_n = \frac{1}{5}a$, $n_e = 10^{19}$ m^{-3} which are the same parameters as we calculated the values in Table 1 in Ref. 1. The results are shown in Table 1 which tells the similar results as described in Ref. 1. That is, it is evident that JT-60 and ASDEX have higher thresholds than the other machines.

Arriving up to this point, it is easy to illustrate the same figure as Fig. 3 in Ref. 1 at $\Delta r \simeq -3.5$ cm to visualize L-H transition. The result is Fig. 4 which is already referred as a convenient example of Eq. 21 as a function of T_e. In Fig. 4, L-point indicates the actual value calculated from Eq. (21) in L-mode plasma, corresponding to L-point in Fig. 3 in Ref. 1. $D_{L\text{-mode}}$-curve shows Eq. (21) as a function of T_e with the other parameters (r_n, n_e, I_p, etc.) fixed on the values at L-point. Therefore, if T_e-rise exceeds

the maximum point (~ 280 eV) enough to reach ~400 eV, predicted from Eq. (29), L-H transition can be expected to occur. We should omit the following occurrence because it is only the repetition of Ref. 1.

In the last place, we try to calculate n_{th} which limits the lowest density triggering the L to H transition, as we did in Ref. 1.* The procedure is same as it is in Ref. 1, so we omit it only to show the final result as follows;

$$r_n > 9.8 \times 10^5 \frac{a^2[1-\frac{r^2}{2a^2}]\varepsilon^{3/2}B}{A^{1/2} I_p} \quad (\equiv r_n^{th}) \tag{30}$$

or

$$n_e > 4.9 \times 10^5 \frac{a^3 \varepsilon^{1/2} B}{A^{1/2} I_p R} \left|\frac{dn_e}{dr}\right| \quad (= n_{th}) \tag{31}$$

where the units are MKS and $j = j_o(1-\frac{r^2}{a^2})$ and $r \simeq a$ are assumed.

This result shows some interesting features about B, R, a^2 and I_p. In Ref. 1, it is found that $n_{th} \propto B^{19/36} I_p^{-5/12}$, while Eq. (31) indicates $n_{th} \propto B/I_p$. As easily traced, it is found that this difference is caused by the part of $(r_n/\rho_s)^{1/3} a^3/r r_n^2$ in Eq. (15) of D_H which is replaced by $[1/<k_\theta \rho_s>]^{1/\beta+X_o}$ in Eq. (21). It is the same cause as in the case of the discussions about the differences of r_n-dependence between Eq. (26) and Eq. (14) in Ref. 1. In Eq. (31), n_{th} is proportional to B. That is more favorable with the experimental result by JET[6] than the result shown in Ref. 1, though it is premature to decide which result should be preferrable experimentally because both equations include dn_e/dr term which requires the close observatory data of $n_e(r)$ at $r \sim a$.

One more interesting remark with regard to Eq. (31) is concerned with the term of a^2B/RI_p which is related to q_a-value. Then we rewrite n_{th} of Eq. (31) as

---

* In Ref. 1, we erroneously omit $R^{1/2}$ in the numerator in Eq. (39) in Ref. 1, therefore, Eqs. (41)-(43) should add the term $R^{17/36}$ in the denominator. This fact modifies some numerical results referred in Ref. 1, though the kernel of the discussions developed there is not hurt.

$$n_{th} \simeq 0.1 \frac{a\, q_a\, \varepsilon_a^{1/2}}{A^{1/2}} \left|\frac{dn_e}{dr}\right| \tag{32}$$

$$\text{or} \quad r_n^{th}/a \cong 0.1\, q_a\, \varepsilon_a^{1/2} / A^{1/2} \ . \tag{33}$$

This relation is amazingly simple and suggests that only three quantities (q_a, ε_a, A) decides r_n^{th}/a and small q_a and ε_a as well as large A should be preferrable to make r_n^{th}/a as small as possible in order to get the advantage of the broad effective region of $r_n/a \geq r_n^{th}/a$ to obtain H-mode.

4. Concluding Remarks

Being motivated by the findings of the common natures of the several forms of the diffusion coefficients having been obtained by several authors[1~4], we induce the unified form Eq. (21) which succeeds to represent the turbulence strength in the power-dependences and the inverse of the adiabaticity can be adopted as a measure to represent the turbulence strength to form both the parts of the base and the power. Though the pseudo-classical type can be approximately consistent with Eq. (21) numerically in the adiabatic region of $X \leq 0.1$ as shown in Fig. 1, the parameter dependences vary in accord with the functional form of Eq. (21). Therefore, in such a case as L-H transition which seems to be caused by a steep rise of T_e, the diffusion coefficient should be treated as a function of T_e, not as a function of X. This fact leads to that Eq. (21) increases as T_e increases and reaches the maximum point, then decreases steeply as T_e goes up more. This picture is quite same as presented in Ref. 1. Therefore, when all the diffusion coefficients ever discovered by several authors are combined into a unified form of Eq. (21), it is easily found to reinforce the model of L-H transition presented in Ref. 1, and be able to give the thresholds of T_{th} and n_{th} by applying the similar procedure as we did in Ref. 1, though the forms of both T_{th} and n_{th} are found to be a little different from those in Ref. 1., expecially with respect to r_n, n_e on T_{th} and B, I_p on n_{th}. But, as previously pointed out, the discrepancy originally results from the differences of the treatments of the nonlinearity part of the system, so that it cannot but still remain to be an open question in the future.

The comparison with the experimental data and the essential parts of L-H transition, such as the formation of the dip of the diffusion coefficient or the enhancement effect of the density gradient dependences, etc. are fairly omitted, because the most parts become only the retelling of the discussions in Ref. 1.

Acknowledgements

The author would be grateful to Dr. Maeda, Manager of our laboratory, who gave the author the continuous encouragement and discussions to this research.

References

1) H. Aikawa; JAERI-M 89-217
2) B.B. Kadomtsev and O.P. Pogutse; Reviews of Plasma Physics vol. V, P249
3) P.W. Terry and P.H. Diamond; Phys. Fluids 28, ('85) 1419
4) R.E. Waltz; Phys. Fluids 28, ('85) 577,
R.E. Waltz, R.R. Domingues, S.K. Wong, P.H. Diamond, G.S. Lee, T.S. Hahm and N. Mattor; in Proc. 11th International Conference on Plasma Physics and Controlled Nuclear Fusion Research, 13-20 Nov. 1986, Kyoto, Japan, vol. I, P345,
R.R. Domingues, and R.E. Waltz; Nuclear Fusion 27, ('87) 65
5) K. Lackner et al.; in Proc. 10th Int. Conf. on Plasma Physics and Cont. Nucl. Fusion Research, London, 12-19 Sept. ('84) vol. I, P319
6) JET Team (presented by M. Keilhacker); in Proc. 12th Int. Conf. on Plasma Physics and Cont. Nucl. Fusion Research, Nice, 12-19 Oct. ('88) vol. I, P159

Acknowledgements

The author would be grateful to Dr. Maeda, Manager of our laboratory, who gave the author the continuous encouragement and discussions to this research.

References

1) H. Aikawa; JAERI-M 89-217
2) B.B. Kadomtsev and O.P. Pogutse; Reviews of Plasma Physics vol. V, P249
3) P.W. Terry and P.H. Diamond; Phys. Fluids 28, ('85) 1419
4) R.E. Waltz; Phys. Fluids 28, ('85) 577,
R.E. Waltz, R.R. Domingues, S.K. Wong, P.H. Diamond, G.S. Lee, T.S. Hahm and N. Mattor; in Proc. 11th International Conference on Plasma Physics and Controlled Nuclear Fusion Research, 13-20 Nov. 1986, Kyoto, Japan, vol. I, P345,
R.R. Domingues, and R.E. Waltz; Nuclear Fusion 27, ('87) 65
5) K. Lackner et al.; in Proc. 10th Int. Conf. on Plasma Physics and Cont. Nucl. Fusion Research, London, 12-19 Sept. ('84) vol. I, P319
6) JET Team (presented by M. Keilhacker); in Proc. 12th Int. Conf. on Plasma Physics and Cont. Nucl. Fusion Research, Nice, 12-19 Oct. ('88) vol. I, P159

Table 1 Threshold values (T_{th}^{P}) of the Tokamak devices, calculated from Eq. (29)

Devices / Threshold Temperature	JT-60	JET	DIII-D	ASDEX	JFT-2M
	a = 0.9m R = 3.0m B = 4.5T I_p = 2.8MA	a = 1m R = 2.8m B = 2.2T I_p = 3MA	a = 0.55m R = 1.7m B = 2.1T I_p = 1.2MA	a = 0.4m R = 1.6m B = 2.2T I_p = 0.32MA	a = 0.3m R = 1.3m B = 1.2T I_p = 0.2MA
T_{th}^{P} (eV)	~ 350	~ 190	~ 180	~ 440	~ 250

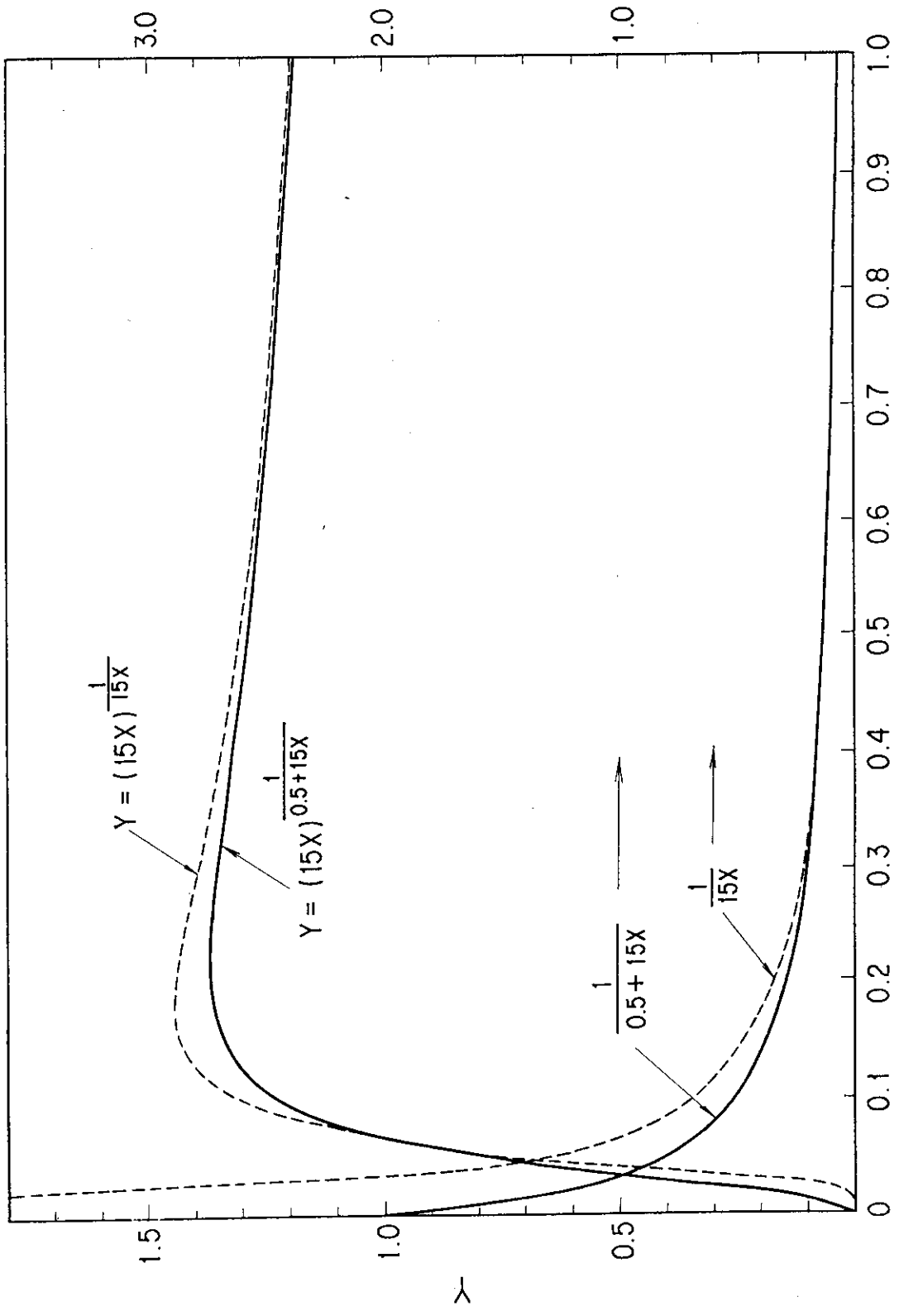

Fig. 1 Functions $Y = (15X)^{\frac{1}{0.5+15X}}$ and $Y = (15X)^{\frac{1}{15X}}$, also showing the power parts $\frac{1}{0.5+15X}$ and $\frac{1}{15X}$

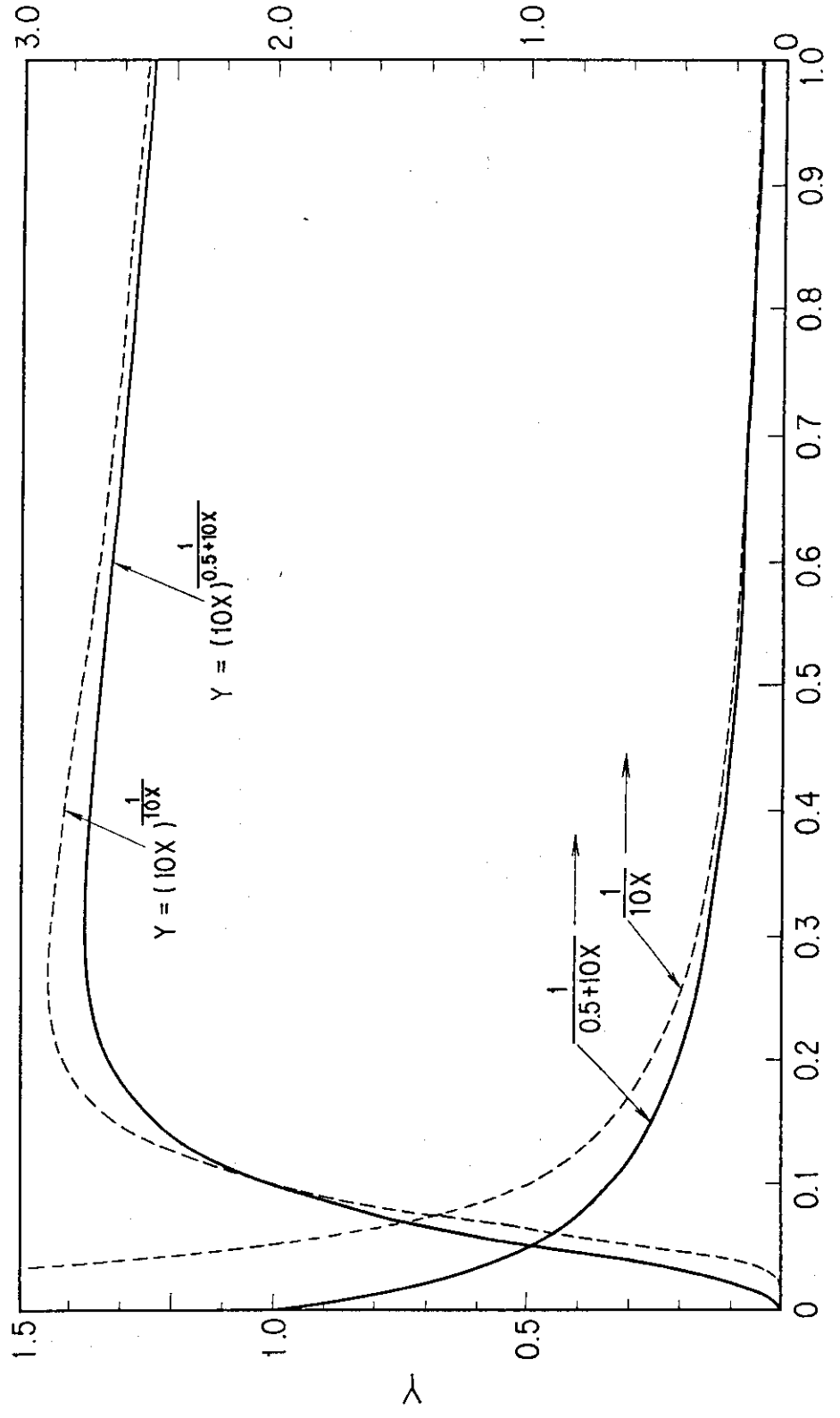

Fig. 2 Functions $Y = (10X)^{\frac{1}{0.5+10X}}$ and $Y = (10X)^{\frac{1}{10X}}$, also showing the power parts $\frac{1}{0.5+10X}$ and $\frac{1}{10X}$

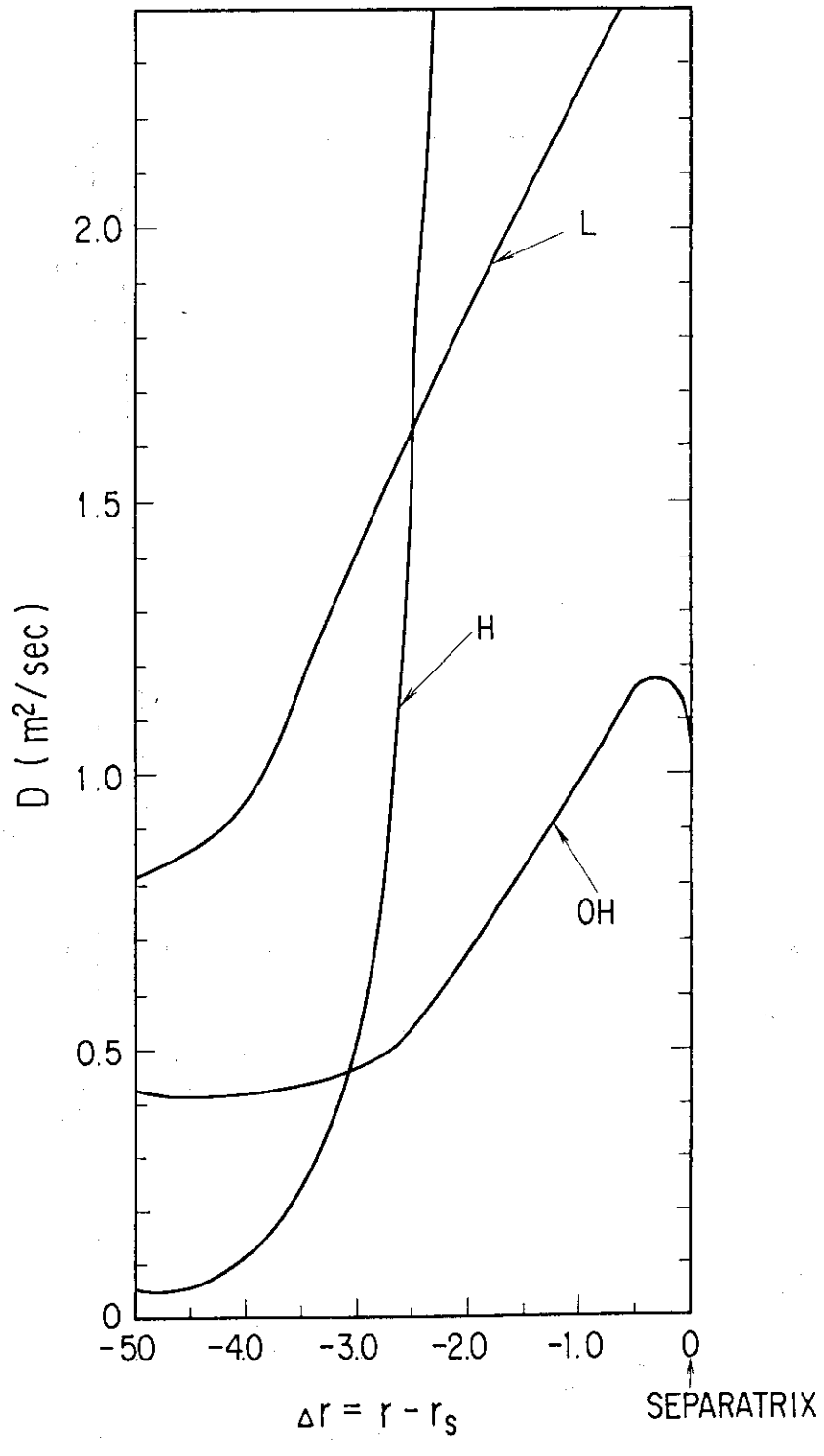

Fig. 3 Diffusion coefficients calculated from Eq. (21) in the cases of OH, L-mode and H-mode plasma of ASDEX-data[5)]

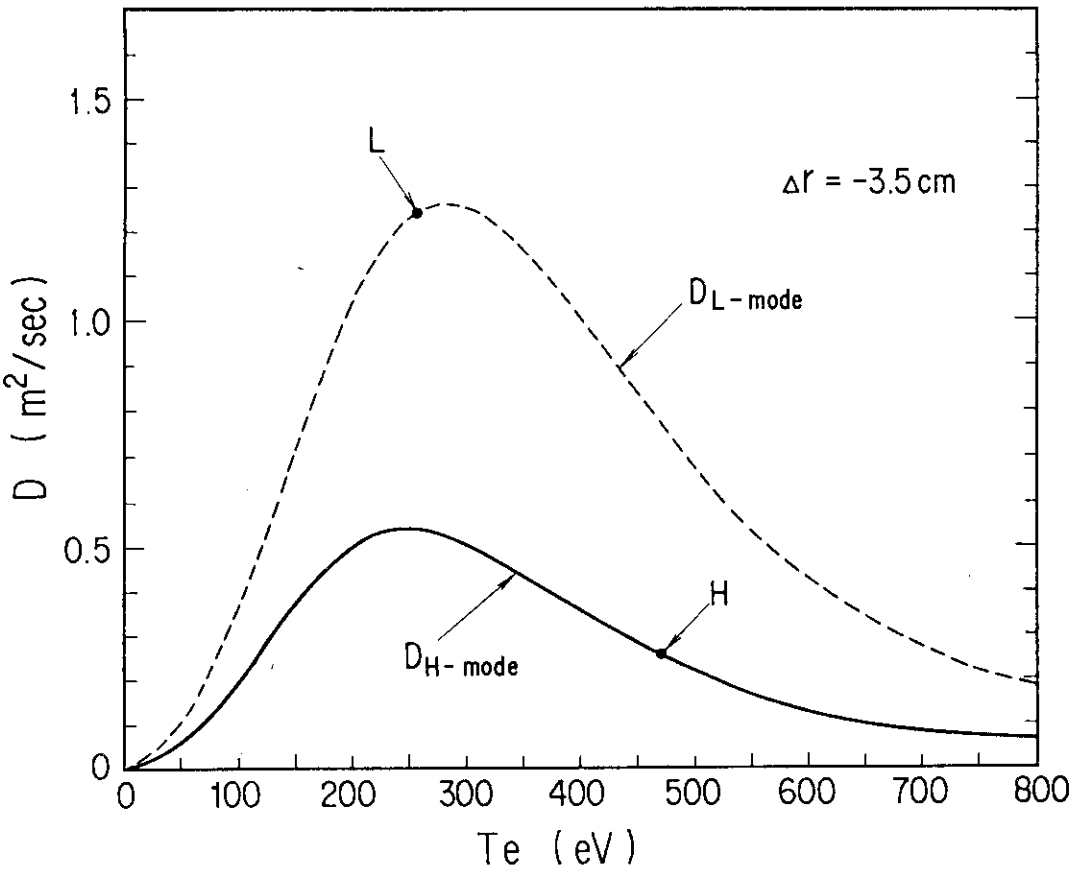

Fig. 4 Diffusion coefficients calculated from Eq. (21) as a function of T_e at $\Delta r = -3.5$ cm in the cases of L-mode and H-mode plasma corresponding to the data in Fig. 3